Int J Thermophys (2008) 29:664–677
DOI 10.1007/s10765-008-0389-x

A Steady-State Apparatus to Measure the Thermal Conductivity of Solids

Giovanni A. Longo

Received: 26 November 2007 / Accepted: 6 February 2008 / Published online: 29 February 2008

Abstract This paper presents a steady-state apparatus to measure the thermal conductivity of solids based on the use of heat flux sensors. The uncertainty assessment of the experimental apparatus is performed in accordance with the ISO "Guide to the Expression of Uncertainty in Measurement" (GUM): the combined standard uncertainty ($k = 1$) with reference to the properties of Pyrex Glass CRM 039 at 20°C is ±1.9%. The standard uncertainty has also been assessed in the measurement range from 0.1 to 10 $\mathrm{W \cdot m^{-1} \cdot K^{-1}}$. The experimental apparatus has been used to measure the certified reference material Pyrex Glass CRM 039 in the temperature range from 3.1 to 60.3°C: the standard deviation ($k = 1$) between the experimental measurements and the certified values is ±1.1% with a maximum deviation of 2.4%. Reasonable agreement is found between the uncertainty assessment and the experimental validation.

Keywords ISO GUM · Reference material · Standard uncertainty · Steady-state method · Thermal conductivity

1 Introduction

The most widespread techniques to measure the thermal conductivity and thermal diffusivity of solids are generally based on non-steady-state approaches such as the transient hot-wire (THW), the transient hot-strip (THS), the transient plane-source (TPS), or the laser-flash (LF) methods.

G. A. Longo (✉)
Department of Management and Engineering, University of Padova,
Str.lla S.Nicola, 3, 36100 Vicenza, Italy
e-mail: tony@gest.unipd.it

In the THW, THS, or TPS methods, a thin metal wire, a rectangular metal strip, or a fin metal strip in the shape of a bifilar spiral clamped between two sample halves, acts simultaneously as a resistive heat source and as a thermometer, whereas the surroundings serve as a heat sink at constant temperature. The thermal conductivity and thermal diffusivity of the sample may be directly derived from the temperature rise of the wire or the strip. The typical standard uncertainty ($k = 1$) of a THS apparatus assessed against the reference material CRM 039 (Pyrex glass) is $\pm 2.5\%$ for the thermal conductivity and $\pm 11\%$ for the thermal diffusivity [1], whereas the typical standard uncertainty ($k = 1$) of a THW apparatus against the same reference material is $\pm 2.9\%$ and $\pm 15\%$, respectively [2].

In the LF method the front face of a small disk-shaped sample receives a pulse of radiant energy from a laser or a flash lamp: the thermal diffusivity of the sample is computed from the temperature response of the opposite (rear) face of the sample. The standard uncertainty ($k = 1$) of an LF apparatus evaluated with reference to the properties of several materials (Pyroceram 9606, Armco iron, Austenitic steel) ranges from $\pm 1.5\%$ to $\pm 2.5\%$ for the thermal diffusivity [3,4]. The simplicity and speed of the measurement and the wide range of applicability are the main advantages of the transient techniques.

Although the usage of transient techniques has increased substantially in recent years, steady-state techniques such as the guarded hot-plate (GHP) technique are still widely used for the measurement of thermal conductivity. These techniques, based directly on Fourier's law, require only measurements of base quantities such as length, temperature, electrical power, etc. Therefore, they can be used for traceability reasons and certification of reference materials. The standard uncertainty ($k = 1$) of a typical GHP apparatus is around ± 1.0 to $\pm 1.5\%$ for thermal conductivities in the measurement range from 0.02 to 6 $\mathrm{W \cdot m^{-1} \cdot K^{-1}}$ [5].

In addition to the steady-state and the transient techniques, a third class of measuring methods known as the quasi-steady-state (QSS) technique is also available. This technique is applied by adding a thermometer to a conventional transient hot-wire (THW) or transient hot-strip (THS) arrangement at a known distance from the wire or the strip. The thermal conductivity may be directly derived from the temperature difference between the thermometer and the wire or the strip that becomes constant after a short settling time. The same result is also obtained by measuring the temperature difference between two different stations of a THW or THS arrangement by using two individual thermometers placed at different radial distances from the wire or the strip. In this way it is possible to generate a steady-state temperature response with a transient operating apparatus. The standard uncertainty ($k = 1$) of a QSS apparatus evaluated with reference to the properties of the material PMMA (polymethyl methacrylate) is $\pm 1.9\%$ for the thermal conductivity [6].

This paper presents a steady-state apparatus to measure the thermal conductivity of solids based on the use of heat flux sensors. The uncertainty of the apparatus has been assessed in accordance with the ISO Guide to the Expression of Uncertainty in Measurement (GUM) [7]. The apparatus has also been used to measure the certified reference material Pyrex Glass CRM 039 [8].

2 Experimental Apparatus and Procedures

The experimental apparatus (see Fig. 1) consists of one hot and one cold plate placed inside a structure working under vacuum. The specimen is a cylinder 25 mm in diameter and 20 mm in thickness, placed between the upper hot plate and the lower cold plate and instrumented with a T-type differential thermocouple (uncertainty within ± 0.05 K ($k = 2$)) and two heat flux sensors (uncertainty within $\pm 5\%$ of the measured value ($k = 2$)). The heat flux sensors, manufactured by TNO [9], are each comprised of a thin disk of epoxy resin in which a thermopile is encapsulated. These heat flux sensors have a limited temperature range, from -20 to 90°C; however, it is possible

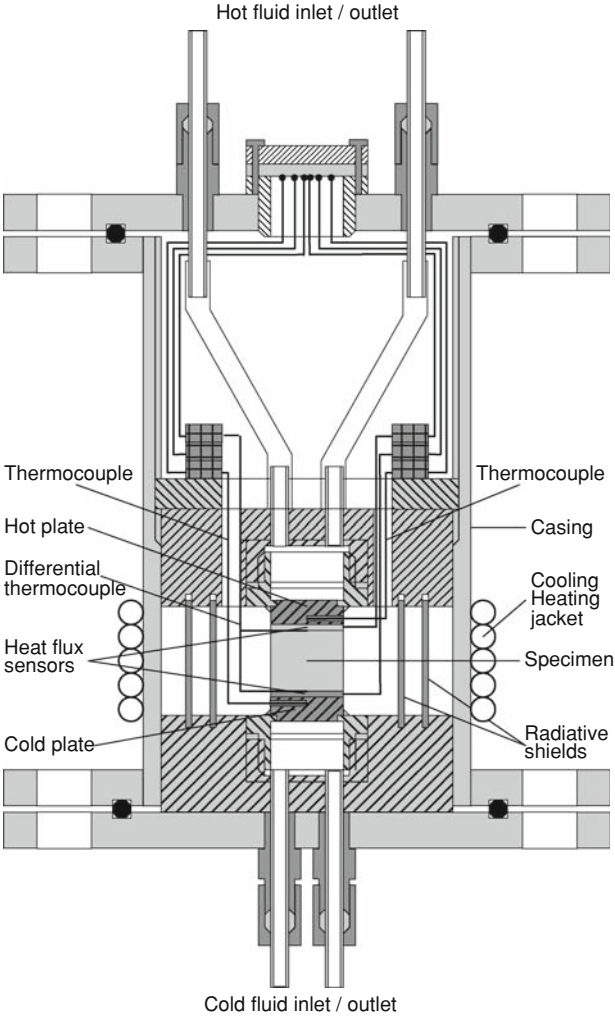

Fig. 1 Schematic view of the experimental apparatus

to also use heat flux sensors made of silicone rubber which have a wider temperature range, from −20 to 250°C.

The hot and cold plates are thermostated by the circulation of fluids coming from two baths (uniformity within ±0.01 K, stability within ±0.01 K) and instrumented with T-type thermocouples (uncertainty within ±0.1 K ($k = 2$)).

The differential thermocouple gives the temperature difference ΔT across the specimen, whereas the heat flux sensors measure the heat fluxes q_{in} and q_{out} at the specimen inlet and outlet, while the thermocouples provide the temperatures T_{hot} and T_{cold} of the plates. The direct measurement of the temperature difference ensures a better accuracy than the separated measurement of the cold- and hot-plate temperatures which is normally carried out in the GHP apparatus.

The system is equipped with two concentric cylindrical radiative shields to reduce the radiative heat exchange and is placed inside a structure working under vacuum to prevent convective heat exchange. Moreover, a cooling/heating jacket, fed with fluid coming from a third bath (uniformity within ±0.01 K, stability within ±0.01 K), controls the temperature of the casing wall to minimize the temperature difference and therefore the radiative heat exchange with the outside surface of the specimen. A vacuum pressure gauge monitors the absolute pressure inside the casing. All the readings, except that of the differential thermocouple, are scanned and measured by a data acquisition system consisting of a 20-channel switch unit and a $6\frac{1}{2}$-digit digital multimeter (uncertainty within ±2.7 μV ($k = 2$)). The reading of the differential thermocouple is scanned and measured by a $7\frac{1}{2}$-digit nanovolt meter equipped with a built-in low-noise two-channel scanner (uncertainty within ±0.27 μV ($k = 2$)). Table 1 gives the main features of the different devices in the experimental apparatus.

Before starting each measurement, the hot and cold baths are set at pre-fixed temperatures and the structure is evacuated by a volumetric vacuum pump. The temperature difference between the hot and cold baths is set between 10 and 40 °C depending on the thermal conductivity of the material to be tested. The absolute pressure inside the casing during measurements is always lower than 10 Pa (10^{-1} mbar). The hot and cold plates and the cooling/heating jacket are fed with the fluids coming from the baths. The readings of the thermocouples, the heat flux sensors, and the vacuum pressure gauge are scanned by the data acquisition system. The temperature of the fluid in

Table 1 Specification data of the different devices

Device	Uncertainty/stability ($k = 2$)	Range
Thermocouple	±0.10 K	−50/+250°C
Diff. thermocouple	±0.05 K	−50/+250°C
Heat flux sensor	±5% of the measured value	−20/+90°C
Acquisition system	±2.70 μV	0/100 mV
Nanovolt meter	±0.27 μV	0/100 mV
Ice-point reference	±0.02 K	0/40°C
Bath	±0.01 K	−20/+200°C

the cooling/heating jacket is adjusted to minimize the difference between the heat fluxes q_{in} and q_{out} at the specimen inlet and outlet and therefore the radiative heat exchange between the specimen and the casing. The final misbalance between inlet and outlet heat fluxes in the experimental tests is always less than 2%. Once temperature, pressure, and heat flux steady-state conditions are achieved, all the quantities are recorded for a set time (generally 1 h), and the average value during this time is computed for each recorded measurement.

It should be noted that the present apparatus is more compact than traditional steady-state apparatus such as GHP, and, therefore, it takes less time to achieve steady-state condition and to carry out the measurement.

Assuming negligible contribution of radiative and convective heat exchange, the thermal conductivity of the specimen can be computed by Fourier's law as follows:

$$\lambda = qH/\Delta T \tag{1}$$

where $q = (q_{\text{in}} + q_{\text{out}})/2$ is the average heat flux through the specimen, H is the specimen thickness, and ΔT is the temperature difference across the specimen.
The thermal conductivity is then related to the mean temperature $T_{\text{m}} = (T_{\text{hot}} + T_{\text{cold}})/2$ between the hot and cold plates.

3 Uncertainty Assessment

The uncertainty $u(y)$ is the parameter, associated with the result of a measurement y, that characterizes the dispersion of the values that could reasonably be attributed to the measured Y. The ISO GUM selects the square root of the variance $u^2(y)$ to quantify the scatter of the measurement and denotes this parameter as the "standard uncertainty." In most cases, the measurement y (output measurement) is determined indirectly from N other measurements x_i (input measurements) on the basis of a functional relationship $y = f(x_i)$. The combined variance $u_{\text{c}}^2(y)$ of the output measurement y may be derived from the variance $u^2(x_i)$ of the input measurements x_i by the Gaussian law of propagation of variance as follows:

$$u_c{}^2(y) = \Sigma_{i=1,N}(\partial f/\partial x_i)^2 u^2(x_i) \tag{2}$$

where $(\partial f/\partial x_i)$ are the sensitivity coefficients. The combined standard uncertainty $u_{\text{c}}(y)$ of an indirect measurement is equal to the square root of the combined variance $u_{\text{c}}^2(y)$. The expanded uncertainty $U(y)$ of a measurement is obtained by multiplying the combined standard uncertainty $u_{\text{c}}(y)$ by a coverage factor k to obtain the required level of confidence.

The ISO GUM offers two alternative procedures for the determination of the variance of the input measurements $u^2(x_i)$: Type A and Type B methods. The Type A method is based on a purely statistical analysis of a series of observations. The Type B method is based on scientific judgment using all available relevant information, including previous measurement data, manufacturer's specifications, data provided in

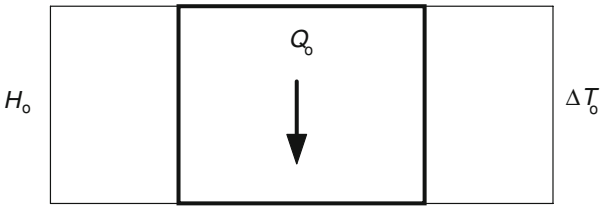

Fig. 2 Ideal model

calibrations, etc. The steps to be followed for evaluating and expressing the uncertainty of a measurement may be summarized as follows:

(a) Formulation of the functional relation between output measurement y and input measurements x_i (ideal model);
(b) Correction to ideal model (real model);
(c) Determination of all sources of uncertainty (uncertainty budget);
(d) Evaluation of the variance of the input measurements $u^2(x_i)$;
(e) Computation of the combined standard uncertainty $u_c(y)$ of the output measurement;
(f) Computation of the expanded uncertainty U of the output measurement.

In the ideal model (see Fig. 2), a one-dimensional conductive heat flow rate Q_o goes through a cylindrical sample of homogeneous and isotropic material with cross-sectional area A_o and thickness H_o when a temperature difference ΔT_o is applied between the opposite faces of the sample.
According to the ideal model, the thermal conductivity of the material is

$$\lambda_o = (Q_o H_o)/(A_o \Delta T_o) \tag{3}$$

The ideal model needs some corrections to account for experimental deviations from perfect behavior (experimental errors). The main sources of experimental errors are

1. Radiative heat exchange—In the experimental apparatus there is radiative heat exchange between the outer surface of the specimen and the casing which produces a deviation from perfect one-dimensional conductive heat flow through the specimen (see Fig. 3). The real heat flow is three-dimensional, and the component along the longitudinal axis of the specimen changes continuously from the inlet (upper surface) to the outlet (lower surface). Therefore, the computation of the thermal conductivity must be referred to the average value of the heat flow rate through the specimen:

$$Q_{ave} = (1/H) \int_O^H Q \mathrm{d}z \tag{4}$$

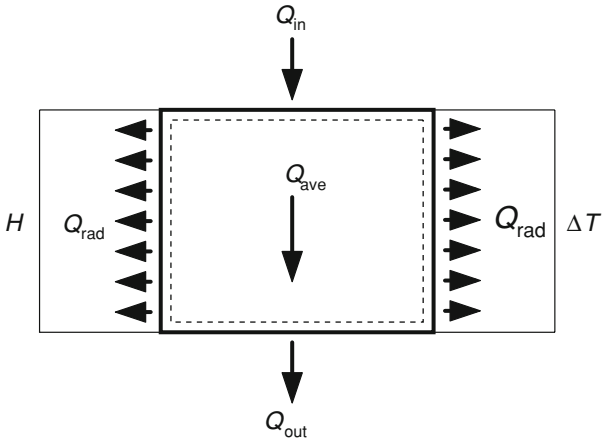

Fig. 3 Real model

The average value of the heat flow rate Q_{ave} differs with the arithmetic mean value between the inlet and outlet,

$$Q_{\text{arith.mean}} = (Q_{\text{in}} + Q_{\text{out}})/2, \tag{5}$$

due to non-linearity of the radiative heat exchange. To evaluate the discrepancy between the average value and the arithmetic mean value; the conductive heat exchange through the specimen; and the radiative heat exchange between the specimen, the radiative shields, and the casing have been simulated by finite element method (FEM) analysis. This analysis shows that, when the unbalance between the inlet and the outlet heat flow rates is less than 1%, the maximum difference between the average and arithmetic mean heat flow rates is less than 0.1%. Therefore, the error due to the approximation of the average value with the arithmetic mean value of the heat flow rate through the specimen may be considered negligible.

2. Thermal conduction along the differential thermocouple—There is some conductive heat exchange between the hot and cold surfaces of the specimen through the differential thermocouple:

$$\Delta Q = \lambda_{\text{Const}} A_{\text{Const}} \Delta T / H \tag{6}$$

where A_{Const} and λ_{Const} are the cross-sectional area and thermal conductivity of the constantan wire of the differential thermocouple. This systematic error may be considered negligible as the cross-sectional area of the constantan wire is five orders of magnitude less than that of the specimen.

3. Heat flux sensors–The heat flux sensor presents measurement errors due to the distortion of the heat flow, to differences of the thermoelectric power, and to the thermal expansion of the sensor [9].

4. Differential thermocouple—The differential thermocouple presents measurement errors due to differences of the thermoelectric power and to the contact thermal resistance between junctions and surfaces of the specimen.
5. Thermal expansion of the specimen—The variation of the specimen thickness with temperature may be evaluated as follows:

$$H = H_o[1 + \alpha(T - T_o)] \tag{7}$$

where α is the expansion coefficient of the specimen material and H_o is the thickness of the specimen at the reference temperature T_o.

The real model incorporates all the above corrections as follows:

$$\begin{aligned} &\lambda(T_m) = (Q_{ave}/A)(H/\Delta T) = 1/2(q_{in} + q_{out})(H/\Delta T) \Rightarrow \\ &\lambda(T_m) = 1/2(q_{in} + q_{out})H_0[1 + \alpha(T_m - T_0)]/\Delta T \end{aligned} \tag{8}$$

The uncertainty of the apparatus has been assessed with reference to the properties of Pyrex Glass CRM 039 [8] at 20°C: Table 2 gives the properties considered in the computation.

The combined variance of the thermal conductivity measurement is

$$\begin{aligned} u_c^2(\lambda) = {} & (\partial\lambda/\partial q_{in})^2 u^2(q_{in}) + (\partial\lambda/\partial q_{out})^2 u^2(q_{out}) + (\partial\lambda/\partial H_o)^2 u^2(H_o) \\ & + (\partial\lambda/\partial\Delta T)^2 u^2(\Delta T) \end{aligned} \tag{9}$$

The sensitivity coefficients are

$$(\partial\lambda/\partial q_{in}) = \frac{1}{2} H_o[1 + \alpha(T_m - T_o)]/\Delta T \tag{10}$$

$$(\partial\lambda/\partial q_{out}) = \frac{1}{2} H_o[1 + \alpha(T_m - T_o)]/\Delta T \tag{11}$$

Table 2 Data for the uncertainty assessment

Material	Pyrex glass CRM 039
Working temperature	20°C
Thermal conductivity	$1.13\,W \cdot m^{-1} \cdot K^{-1}$
Heat flux	$565\,W \cdot m^{-2}$
Temperature difference	10°C
Specimen thickness	20 mm
Specimen diameter	25 mm
Specimen cross-sectional area	$490.86\,mm^2$

$$(\partial\lambda/\partial H_{\mathrm{o}}) = \frac{1}{2}(q_{\mathrm{in}} + q_{\mathrm{out}})[1 + \alpha(T_{\mathrm{m}} - T_{\mathrm{o}})]/\Delta T \tag{12}$$

$$(\partial\lambda/\partial \Delta T) = -\frac{1}{2}(q_{\mathrm{in}} + q_{\mathrm{out}})H_{\mathrm{o}}[1 + \alpha(T_{\mathrm{m}} - T_{\mathrm{o}})]/\Delta T^2 \tag{13}$$

The uncertainties and variances of the input measurements are

(1) Heat flux measurement. The manufacturer of the heat flux sensor states an uncertainty ($k = 2$) within ±5% of the measured value. The uncertainty of the measurement of the output signal from the heat flux sensor has negligible effect on the combined uncertainty of the heat flux measurement. Therefore, the absolute standard uncertainty ($k = 1$) and the variance of the heat flux measurement are assumed equal to those of the heat flux sensor:

$$u(q) = [0.05 \times 565\,\mathrm{W \cdot m^{-2}}]/2 = \pm 14.125\,\mathrm{W \cdot m^{-2}} \tag{14}$$

$$u^2(q) = 199.5\,\mathrm{W^2 \cdot m^{-4}} \tag{15}$$

(2) Specimen thickness measurement. The uncertainty ($k = 2$) in the measurement of the reference thickness is $\pm 1.0 \times 10^{-4}$ m. Therefore, the standard uncertainty ($k = 1$) and the variance are

$$u(H_{\mathrm{o}}) = \pm 5.0 \times 10^{-5}\mathrm{m} \tag{16}$$

$$u^2(H_{\mathrm{o}}) = 2.5 \times 10^{-9}\mathrm{m}^2 \tag{17}$$

The thermal expansion of the Pyrex glass is negligible ($\alpha_{\mathrm{Pyrex}} = 3.3 \times 10^{-6}\,\mathrm{K}^{-1}$ at 20°C)

(3) Temperature difference measurement. The uncertainty ($k = 2$) of the differential thermocouple, including the whole measuring chain, derived from a statistical analysis of a series of measurements, is ±0.05 K. Therefore, the standard uncertainty ($k = 1$) and the variance are

$$u(\Delta T) = \pm 2.5 \times 10^{-2}\mathrm{K} \tag{18}$$

$$u^2(\Delta T) = 6.25 \times 10^{-4}\mathrm{K}^2 \tag{19}$$

Table 3 provides all the data for the uncertainty analysis, such as input quantities with estimated values, sensitivity coefficients, standard uncertainty, variance and output quantity with estimated values, combined variance, and combined standard uncertainty (uncertainty budget). The uncertainty of the heat flux measurement has the largest influence on the combined uncertainty, whereas the uncertainties of the thickness

Table 3 Uncertainty Budget

Quantity	Estimated value	Sensitivity coeff. $(\partial f/\partial x_i)$	St. uncertainty $u(x_i)$	Variance $u^2(x_i)$	Comb. Variance $(\partial f/\partial x_i)^2 u^2(x_i)$	Comb. Standard uncertainty
q_{in}	$565\,\text{W}\cdot\text{m}^{-2}$	$1.00\times10^{-3}\,\text{m}\cdot\text{K}^{-1}$	$14.125\,\text{W}\cdot\text{m}^{-2}$	$199.51\,\text{W}^2\cdot\text{m}^{-4}$	$1.99\times10^{-4}\,\text{W}^2\cdot\text{m}^{-2}\cdot\text{K}^{-2}$	
q_{out}	$565\,\text{W}\cdot\text{m}^{-2}$	$1.00\times10^{-3}\,\text{m}\cdot\text{K}^{-1}$	$14.125\,\text{W}\cdot\text{m}^{-2}$	$199.51\,\text{W}^2\cdot\text{m}^{-4}$	$1.99\times10^{-4}\,\text{W}^2\cdot\text{m}^{-2}\cdot\text{K}^{-2}$	
H_{o}	$2.0\times10^{-2}\,\text{m}$	$56.5\,\text{W}\cdot\text{m}^{-2}\cdot\text{K}^{-1}$	$5.0\,10^{-5}\,\text{m}$	$2.5\,10^{-9}\,\text{m}^2$	$3.19\times10^{-5}\,\text{W}^2\cdot\text{m}^{-2}\cdot\text{K}^{-2}$	
ΔT	10.0°C	$-1.13\times10^{-1}\,\text{W}\cdot\text{m}^{-1}\cdot\text{K}^{-2}$	$2.5\,10^{-2}\,\text{K}$	$6.25\,10^{-4}\text{K}^2$	$7.98\times10^{-6}\,\text{W}^2\cdot\text{m}^{-2}\cdot\text{K}^{-2}$	
λ	$1.13\,\text{W}\cdot\text{m}^{-1}\cdot\text{K}^{-1}$				$4.39\times10^{-4}\,\text{W}^2\cdot\text{m}^{-2}\cdot\text{K}^{-2}$	$0.021\,\text{W}\cdot\text{m}^{-1}\cdot\text{K}^{-1}$

measurement and temperature difference measurement give relatively small contributions.

The combined standard uncertainty ($k = 1$) to be assigned to the thermal conductivity measurement on Pyrex Glass CRM 039 at 20°C is

$$u(\lambda) = \pm 0.021\ \mathrm{W \cdot m^{-1} \cdot K^{-1}} \tag{20}$$

$$u'(\lambda) = u(\lambda)/\lambda = \pm 1.9\% \tag{21}$$

The corresponding expanded uncertainty for a coverage factor of 2 ($k = 2$) is

$$U(\lambda) = 2u(\lambda) = \pm 0.042\ \mathrm{W \cdot m^{-1} \cdot K^{-1}} \tag{22}$$

$$U'(\lambda) = U(\lambda)/\lambda = \pm 3.8\% \tag{23}$$

The uncertainty of the apparatus has also been assessed in the measurement range from 0.1 to $10\,\mathrm{W \cdot m^{-1} \cdot K^{-1}}$ assuming a constant temperature difference (10°C) for thermal conductivities $0.1 \leq \lambda < 1$ and a constant heat flux ($500\,\mathrm{W \cdot m^{-2}}$) for thermal conductivities $1 \leq \lambda \leq 10$. Figure 4 shows the standard uncertainty ($k = 1$) versus the thermal conductivity. The standard uncertainty is less than ±2% for thermal conductivities less than $3\,\mathrm{W \cdot m^{-1} \cdot K^{-1}}$, whereas for higher thermal conductivities, it increases rapidly due to the uncertainty of the temperature difference measurement. The standard uncertainty is around ±3% for a thermal conductivity of $10\,\mathrm{W \cdot m^{-1} \cdot K^{-1}}$.

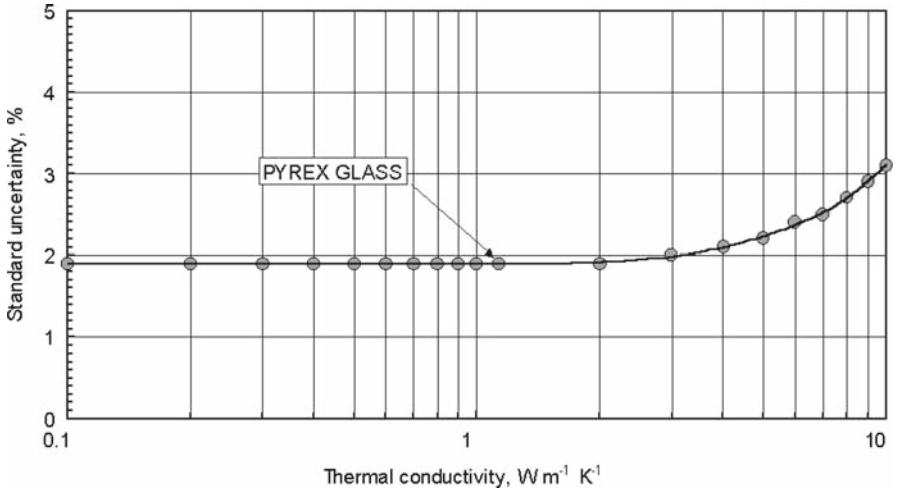

Fig. 4 Standard uncertainty versus thermal conductivity

4 Measurements on a Reference Material

The experimental apparatus has been used for extensive measurements on the certified reference material Pyrex Glass CRM 039; 26 measurements have been carried out in the temperature range from 3.1 to 60.3°C.

The specimen, a cylinder 25 mm in diameter, has been cut from a Pyrex Glass CRM 039 sheet 400 mm × 400 mm having a thickness of (18.96 ± 0.1 mm) ($k = 2$).

The experimental measurements of the thermal conductivity have been compared against the certified values computed by the following relation [8]:

$$\lambda(T) = 1.1036 + 1.659 \times 10^{-3} T - 3.982 \times 10^{-6} T^2 + 6.764 \times 10^{-9} T^3 \quad (24)$$

$$\lambda(\mathrm{W \cdot m^{-1} \cdot K^{-1}}) \qquad -75^\circ\mathrm{C} \le T(^\circ\mathrm{C}) \le 195^\circ\mathrm{C}$$

The uncertainty ($k = 2$) of the certified values is ±1.7%. It must be noted that the certified values and the relative uncertainty refer to the original full sheet, and, therefore, the extrapolation of these values to a smaller specimen cut from the sheet might be suspect.

Figure 5 shows the deviations between the experimental measurements and the certified values. The standard deviation ($k = 1$) is ±1.1% with a maximum deviation of 2.4%.

Thus, reasonable agreement is found between the theoretical uncertainty assessment and the experimental verification.

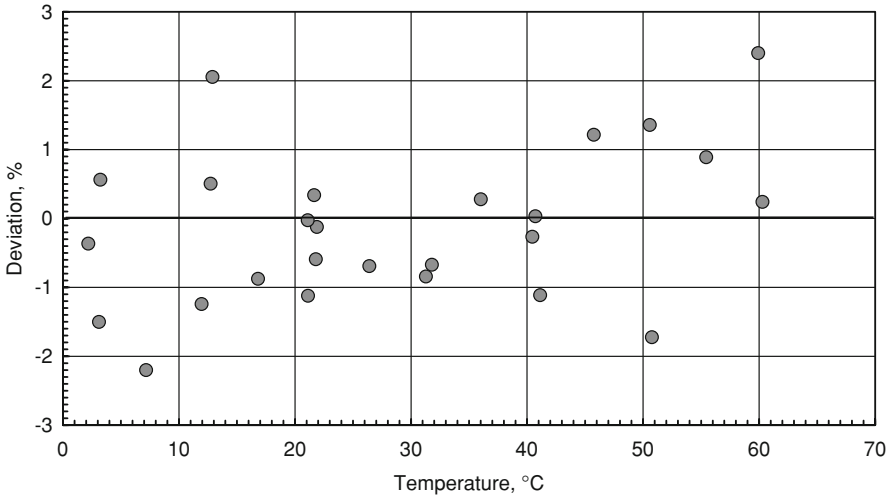

Fig. 5 Comparison between experimental measurements and certified data for Pyrex Glass CRM 039

5 Conclusion

The combined standard uncertainty ($k = 1$), assessed in accordance with ISO GUM, for the thermal conductivity measurement on Pyrex Glass CRM 039 at 20°C is ±1.9%. The standard uncertainty increases rapidly for thermal conductivities larger than $3\,\mathrm{W \cdot m^{-1} \cdot K^{-1}}$ due to the uncertainty of the temperature difference measurement.

The standard deviation ($k = 1$) between the experimental measurements on the reference material Pyrex Glass CRM 039 and the certified values is ±1.1% in the temperature range from 3.1 to 60.3°C.

Reasonable agreement is found between the theoretical uncertainty assessment and the experimental verification.

Nomenclature

A	Specimen cross-sectional area	$\mathrm{m^2}$
H	Specimen thickness	m
k	Coverage factor	
q	Heat flux	$\mathrm{W \cdot m^{-2}}$
Q	Heat flow rate	W
T	Temperature	K
u	Standard uncertainty	
u'	Relative standard uncertainty	
u_c	Combined standard uncertainty	
U	Expanded uncertainty	
U'	Relative expanded uncertainty	
u^2	Variance	
x_i	Input measurement	
X_i	Input quantity	
y	Output measurement	

Greek symbols

α	Expansion coefficient	$\mathrm{K^{-1}}$
Δ	Difference	
λ	Thermal conductivity	$\mathrm{W \cdot m^{-1} \cdot K^{-1}}$

Subscripts

arith.mean	Arithmetic mean
ave	Average
c	Combined
cold	Cold side
hot	Hot side
m	Mean
o	Ideal
in	Inlet
out	Outlet

Acknowledgment This paper is dedicated to Francesco De Ponte who first built at the University of Padova an apparatus to measure the thermal conductivity of insulating materials.

References

1. U. Hammerschmidt, W. Sabuga, Int. J. Thermophys. **21**, 217 (2000)
2. U. Hammerschmidt, W. Sabuga, Int. J. Thermophys. **21**, 1255 (2000)
3. B. Hay, J.R. Filtz, J. Hameury, L. Rongione, Int. J. Thermophys. **26**, 1883 (2005)
4. L. Vozár, W. Hohenauer, Int. J. Thermophys. **26**, 1899 (2005)
5. U. Hammerschmidt, Int. J. Thermophys. **23**, 1551 (2002)
6. U. Hammerschmidt, Int. J. Thermophys. **25**, 1163 (2004)
7. ISO, *Guide to the Expression of Uncertainty in Measurement (GUM)* (ISO, Geneva, 1995)
8. BCR, "Certification report for Pyrex Glass reference material for thermal conductivity between −75 and 195°C (CRM 039)," Commission of European Communities, *Rept. EUR 13358 EN*, Luxembourg (1991)
9. W. Göpel, J. Hesse, J.N. Zemel (eds.), in *Sensors*, vol. 4, Chap. 8, *Heat-Flux Sensors* (VCH Verlagsgesellschaft, Weinheim, Germany, 1990)